Physics Letters A 374 (2010) 4061–4064

Contents lists available at ScienceDirect

Physics Letters A

www.elsevier.com/locate/pla

Tunable band structure effects on ballistic transport in graphene nanoribbons

O. Roslyak [a,*], Godfrey Gumbs [a,c], Danhong Huang [b]

[a] Department of Physics and Astronomy, Hunter College of City University of New York, 695 Park Avenue, New York, NY 10065-50085, USA
[b] Air Force Research Laboratory (AFRL/RVSS), Kirtland Air Force Base, NM 87117, USA
[c] Donostia International Physics Center (DIPC), P. de Manuel Lardizabal, 4, 20018 San Sebastián, Basque Country, Spain

ARTICLE INFO

Article history:
Received 5 June 2010
Accepted 19 June 2010
Available online 5 August 2010
Communicated by V.M. Agranovich

Keywords:
Graphene
Nanoribbons
Ballistic transport

ABSTRACT

Graphene nanoribbons (GNR) in mutually perpendicular electric and magnetic fields are shown to exhibit dramatic changes in their band structure and electron transport properties. A strong electric field across the ribbon induces multiple chiral Dirac points, closing the semiconducting gap in armchair GNRs. A perpendicular magnetic field induces partially formed Landau levels as well as dispersive surface-bound states. Each of the applied fields on its own preserves the even symmetry $E_k = E_{-k}$ of the subband dispersion. When applied together, they reverse the dispersion parity to be odd and gives $E_{\mathrm{e},k} = -E_{\mathrm{h},-k}$ and mix the electron and hole subbands within the energy range corresponding to the change in potential across the ribbon. This leads to oscillations of the ballistic conductance within this energy range.

Recent advantages in the fabrication techniques of graphene nanoribbons (GNR) together with the long electron mean free path have stimulated considerable interest in their potential applications as interconnects in nano circuits. Near the K and K' Dirac points for infinite graphene, the electrons are massless and chiral [1]. The electronic properties of GNR are sensitive to the geometry of their edges and the number of carbon atoms N across the ribbon. The GNR is thus classified as armchair (ANR), zigzag (ZNR) nanoribbons for even N and their counterpart anti-armchair (AANR), anti-zigzag (AZNR) for odd N. The armchair confinement mixes K and K' valleys creating chiral electrons around the Γ point. Chirality is the key ingredient for unimpeded electron transport (Klein effect). Depending on N, modulo 3, the ANR/AANR can be either metallic or semiconducting making them suitable candidates for use as field-effect transistors. In contrast, the zigzag confinement does not mix the valleys but rather intertwine their longitudinal and transverse momenta, creating edges-bound quasiparticles between the K and K' points. For ZNR/AZNR, the electrons are not chiral (in the sense of projection of the pseudo-parity on the particle momentum), and the electron transmission through a potential barrier is determined by the electron pseudo-parity [2]. This quantity redefines the Klein effect as the suppressed transmission through the barrier in ZNR, also known as the valley-valve effect [3]. The latter is the basis for the proposed valley filters. The electron confinement in GNR causes their properties to be quite sensitive to an applied electric [4–6] or magnetic [7–10] field. These changes are reflected in measurable quantities such as the ballistic conductivity and local density of states (LDOS) [11,12].

In this Letter, we report on the individual and combined effects of an electric and magnetic field on the band structure and conductance of GNRs. If only one of the fields is applied, it is well known that the time reversal symmetry[1] [13] of the energy bands for electrons and holes is preserved for all the types of GNRs we listed above. However, the combined effect of an electric and magnetic field on the energy dispersion is to break the time reversal symmetry for both electrons and holes and mix the energy bands. The effect of mixing on the differential conductance and LDOS is presented below and our results are compared to those obtained when only one of the two external fields is applied to an ANR with quantum point contacts as illustrated schematically in Fig. 1. The ribbon is attached to left (L) and right (R) leads serving as infinite electron reservoirs. The R-lead is assumed to be the drain held at chemical potential μ. The L-lead is held at DC biased chemical potential $\mu + eV$ (e is the electron charge and V is the bias potential) and serves as the source. We choose coordinate axes so that the nanoribbon is along the x axis in the xy-plane. Mutually perpendicular static electric field $\mathcal{E}_y$ along the y axis and magnetic field $\mathcal{B}_z$ along the z axis are applied, as shown in Fig. 1.

We calculated the energy bands for graphene with sublattices A and B in the tight-binding model [14,1]. These are then separated

* Corresponding author.
E-mail address: avroslyak@gmail.com (O. Roslyak).

[1] Since we neglect spin, the action of the time reversal operator $\hat{\mathcal{T}}$ amounts to reversing the direction of the wave vector propagation. The even/odd particle energy symmetry may be defined as $E_{n,k} = \pm\hat{\mathcal{T}} E_{n,k} = \pm E_{n,-k}$.

0375-9601/$ – see front matter © 2010 Published by Elsevier B.V.
doi:10.1016/j.physleta.2010.08.003

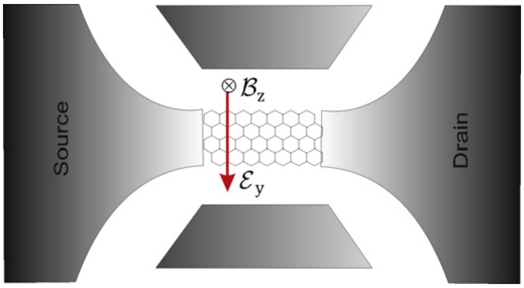

Fig. 1. (Color online.) Schematic of an ANR in the presence of an in-plane electric field $\mathcal{E}$ along the y axis and a perpendicular magnetic field B along the z axis.

into hole $\{h\} = \{1 \leqslant n < N\}$ and electron $\{e\} = \{N \leqslant n < 2N\}$ energy bands. The two component wave function is a normalized $2N$ vector:

$$\langle \Psi(y)|_{n,k} = \begin{pmatrix} \langle \Psi_A(y)|_{n,k} \\ \langle \Psi_B(y)|_{n,k} \end{pmatrix}.$$

Along the ribbon we have a plane wave $\exp(ikx)$, characterized by its wave vector k. The electric field induces a potential across the ribbon $U(y) = e\mathcal{E}_y(y - W/2) = U_0[(y/W) - 1/2]$, where W is the ribbon width and $U_0 = e\mathcal{E}_y W$. This potential is screened by the carriers. The screening potential is found self-consistently by solving the Poisson equation with LDOS as the source. The magnetic field modifies the wave vector as $k \to k - e\mathcal{B}_z y/\hbar$, which amounts to the Peierls phase in the hopping integrals [15]. The magnetic field strength is assumed weak so we could take the energy levels as spin degenerate. The dispersion curves can be experimentally observed via scanning tunneling microscopy [16]. The tunneling current flowing through the microscope tip is proportional to the LDOS given by

$$\mathrm{LDOS}(E, y) = \sum_{n,k} \left|\Psi_{n,k}(y)\right|^2 \delta(E - E_{n,k}). \tag{1}$$

The energy dispersion determines the ballistic charge current I through the ribbon, at temperature T, by

$$\begin{aligned} &I(V, \mu, \mathcal{E}_y, \mathcal{B}_z, T) \\ &\quad = -2e \sum_n \int \frac{dk}{2\pi} v_{n,k}\left[\theta(-v_{n,k}) f^{>}_{n,k}\left(1 - f^{<}_{n,k}\right) \right. \\ &\qquad \left. + \theta(v_{n,k}) f^{<}_{n,k}\left(1 - f^{>}_{n,k}\right)\right], \end{aligned} \tag{2}$$

where $v_{n,k} = dE_{n,k}/d(\hbar k)$ is the carrier group velocity. At $T = 0$, the Fermi function at the source contact is $f^{<}_{n,k} = 1 - \theta(E_{n,k} - \mu - eV)$ and for the drain, we have $f^{>}_{n,k} = 1 - \theta(E_{n,k} - \mu)$. We note that Eq. (2) does not assume any symmetry for the energy dispersion relation. If the energy satisfies $E_{n,k} = E_{n,-k}$, we obtain the well-known Landauer–Büttikker formula [17]. The differential conductance $G(\mu, \mathcal{E}_y, \mathcal{B}_z) = (\partial I/\partial V)_{V=0}$ is determined by the number of right-moving carriers through $v_{n,k}/|v_{n,k}| > 0$ at the chemical potential $E_{n,k} = \mu$. Alternatively, one may take the difference between the local minima and maxima below the chemical potential $E_{n,k} < \mu$ [11].

Our numerical results for the energy bands, LDOS and conductance for semiconducting ANR ($N = 51$) in the presence of an electric and/or magnetic field are presented in Fig. 2. When either only an electric or magnetic field is applied $\mathcal{E}_y\mathcal{B}_z = 0$, the electron/hole energy bands are symmetric with $E_{\mathrm{h},k} = -E_{\mathrm{e},k}$ and time reversal symmetry is satisfied with $E_{n,k} = E_{n,-k}$ around the $k = 0$ Dirac point in Fig. 2(b.1). The latter means that if the time for the particle is reversed, the particle retraces its path along the same electron/hole branch. The LDOS also demonstrates the wave function symmetry with respect to the ribbon center $\mathrm{LDOS}(E, x) = \mathrm{LDOS}(-E, x) = \mathrm{LDOS}(E, -x)$. In accordance with the Landauer–Bütikker formalism, the conductivity demonstrates the familiar staggering pattern. The magnetic field by itself distorts the weak dispersion (n close to N) so that the partially formed Landau levels $E_{n,0} \sim \sqrt{\mathcal{B}_z n}$ shows itself up as the flat parts in the dispersion curves. The lowest Landau level provides the single conducting channel (along the ribbon edges), while the rest are doubly degenerate. When the wave vector evolves from the Dirac point, the degeneracy is lifted and the lowest subband acquires a local minimum. Of these two effects, the first one can be observed in the LDOS, while the second reveals itself as sharp spikes in the conductance as depicted in Fig. 2(b.3). For the high energy subbands, when the radii of the Landau orbits (spread of the wave function in Fig. 2(b.2)) become comparable with the ribbon width, the confinement effects dominate and the spectra become linear in magnetic field with $E_{n,0} \sim \mathcal{B}_z/n$. These subbands are not degenerate.

The main effect which the electric field has on the energy dispersion is to fracture Fermi surface into small pockets for $k \neq 0$, and thereby closing the semiconducting energy gap. These zero energy points, where the group velocity abruptly changes sign, represent new Dirac points, which follows from the chirality of the wave function in their vicinity [18]. The rapid changes in the group velocity cause the appearance of spikes in the conductance near $|\mu| \leqslant U_0/2$ and its step-like pattern is broken. Due to the Dirac symmetry of the problem, the electron-hole band structure remains symmetric. The energy dispersion is not affected by magnetic field at the original Dirac point $k = 0$. Time reversal symmetry also persists. The LDOS shows that at high energies the electric field confines the electrons and holes near opposite boundaries. However, at low energies the LDOS does not change across the ribbon, which is a manifestation of the Zitterbewegung effect (attempt to confine Dirac fermions causes wave function delocalization [1]). With respect to the three cases considered above, we point out that the hallmark of Dirac fermions is the even symmetry of the dispersion with respect to the wave vector, and steams from time reversal symmetry. Even though an attempt to confine them may lead to the broken electron/hole symmetry [19], the wave vector symmetry still persists.

We now turn our attention to the most interesting case when both electric and magnetic fields are applied together. Concurrent action of the electric field dragging force, the Lorentz force and confinement by the ribbon edges *destroys* the Dirac symmetry of the problem so that $E_{n,k} \neq E_{n,-k}$ as shown in Fig. 2(d.1). The dispersion distortion is different for the electrons and holes, so the symmetry between the conduction and valence bands is also broken. On one hand, the partially formed Landau levels get distorted by the confinement due to the electric field in conjunction with the edges. Their degeneracy is also lifted. On the other hand, the magnetic field does not allow formation of additional Dirac points and wave function delocalization. At high energies, where the group velocity is decreased and the drag due to the electric field prevails. The electrons and holes get gathered at the opposite ribbon edges (Fig. 2(d.2)). For lower energies, in the region $|E_{n,k}| \leqslant U_0/2$, the electron/hole dispersions overlap. The electron bands have only local minima, whereas only the hole bands have local maxima. Regardless of the broken Dirac k symmetry of the dispersion, our numerical simulation of the differential conductivity shows that the Landauer–Bütikker expression still applies. Therefore, in the overlapping region $|\mu| \leqslant U_0/2$, the conductivity oscillates since the minimum of the electron band is followed by the maximum on the hole band when the chemical potential grows. As for possible applications of the broken Dirac symmetry, the ribbon, subjected to mutually transverse electric and magnetic fields, may serve as a field-effect transistor with a tunable working point. An interesting feature of our results is that there is not